

# 1 Jet sub-structure and parton shower evolution in 2 p+p and Au+Au collisions at STAR

---

**Raghav Kunnawalkam Elayavalli for the STAR Collaboration\***

Wayne State University, Detroit MI 48201

E-mail: [raghavke@wayne.edu](mailto:raghavke@wayne.edu)

Recent measurements of jet structure modifications at RHIC and LHC highlight the importance of differential measurements to study the nature of jet quenching. Since these jet structure observables are intimately dependent on parton evolution in both the angular and energy scales, measurements are needed to disentangle these two scales in order to probe the medium at different length scales to study its characteristic properties such as the coherence length. To that effect, the STAR collaboration presents fully unfolded results of jet sub-structure observables designed to extract fundamental quantities related to the parton shower via the SoftDrop shared momentum fraction ( $z_g$ ), the groomed jet radius ( $R_g$ ) and the jet Mass ( $M$ ) in p+p collisions at  $\sqrt{s} = 200$  GeV as a function of jet transverse momenta. We also showcase the first measurement of iterative softdrop groomed  $z_g$  and  $R_g$  for first, second and third splits with an initiator prong transverse momenta ranging from 20-25 GeV. In comparing the un-corrected data to our simulation, we are able to look at snapshots of the jet clustering history leading towards an understand of the time evolution of the parton shower. Having established the p+p baseline, we present the first measurement of the jet's inherent angular structure in Au+Au collisions at  $\sqrt{s_{NN}} = 200$  GeV via an experimentally robust observable related to the SoftDrop  $R_g$ : the opening angle between the two leading sub-jets ( $\theta_{SJ}$ ). In Au+Au collisions at STAR, we utilize a specific di-jet selection as introduced in our previous momentum imbalance ( $A_J$ ) measurement and measure both the  $A_J$  and the recoil jet spectra differentially as a function of the angular classes based on the  $\theta_{SJ}$  observable. With such measurements, we probe the medium response to jets at a particular resolution scale and find no significant differences in quenching for jets of different angular scales as given by  $\theta_{SJ}$ .

*13th International Workshop on High-pT Physics in the RHIC/LHC era  
19 - 22 March 2019  
Knoxville, Tennessee, USA*

---

\*Speaker.

### 3 1. Introduction

4 Relativistic ion collisions produce copious amounts of jets due to the hard scatterings between  
 5 quarks and gluons of the colliding nuclei. Recent measurements at both RHIC and LHC along with  
 6 theoretical advancements have shown the importance of studying and measuring the properties of  
 7 these jets both in p+p and in heavy ion collisions (review of jet studies can be found here [1]).  
 8 There are two natural scales that characterize a jet and its evolution: the momentum and the angular  
 9 scales. First generation jet measurements have measured jet quenching in an integrative manner,  
 10 for example via the momentum asymmetry in di-jet events and have further extensively studied the  
 11 momentum dependence via nuclear modification factors and fragmentation functions. Jet-medium  
 12 interaction could further be dependent on the resolution scale or the coherence length of the medium  
 13 which perceives the jet as a singular radiating object or a multi-prong object [2].

### 14 2. Jet sub-structure in p+p Collisions

15 In order to differentially study energy loss in the QGP medium, the jet structure in vacuum  
 16 has to be first understood at both momentum and virtuality scales related to the DGLAP splitting  
 17 functions [3] that govern parton evolution. SoftDrop [4] is an algorithm with which one can extract  
 18 such scales experimentally utilizing its procedure of walking backwards in the Cambridge/Aachen  
 19 clustering tree until two sub-jets satisfy  $z = \frac{\min(p_{T,1}, p_{T,2})}{p_{T,1} + p_{T,2}} > z_{cut} (\Delta R/R)^\beta$  where  $z_g$  and  $R_g$  are the  $z$   
 20 and  $\Delta R$  upon termination of the algorithm with  $z_{cut} = 0.1$  and  $\beta = 0$ . It was shown that for such  
 21 choices of  $z_{cut}, \beta$  the SoftDrop  $z_g$  distribution converges to the vacuum DGLAP splitting functions  
 22 for  $z > z_{cut}$  in a ‘‘Sudakov-safe’’ manner [5]. The invariant jet mass is also measured as a function  
 23 of jet  $p_T$  since it is dependent on the virtuality scale set by the parton shower.

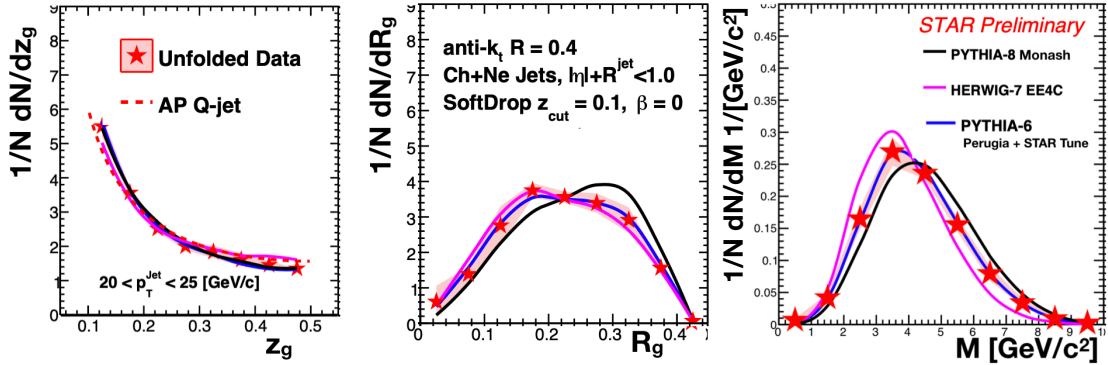


**Figure 1:** Fully unfolded measurement of the SoftDrop groomed sub-jet shared momentum fraction ( $z_g$ ), the groomed jet radius ( $R_g$ ) and the jet mass in p+p collisions at  $\sqrt{s} = 200$  GeV for jets with  $20 < p_T < 25$  GeV/c.

24 The p+p data for the jet sub-structure measurements were collected with the STAR detec-  
 25 tor [6] during the 2012 run at  $\sqrt{s_{NN}} = 200$  GeV. Jets are reconstructed from charged tracks in the  
 26 Time Projection Chamber (TPC) and energy depositions in the Barrel ElectroMagnetic Calorimeter  
 27 (BEMC) using the anti- $k_t$  algorithm as implemented in the FastJet package [7], hereafter referenced

28 as Ch+Ne jets. For additional details regarding event/track/tower quality selections, please refer  
29 to [8, 9, 10].

30 The  $z_g$ ,  $R_g$  and  $M$  distributions versus jet  $p_T$  are corrected using two-dimensional bayesian  
31 unfolding as implemented in the RooUnfold package [11, 12] with four iterations. The response  
32 matrix is created from a PYTHIA-6 (Perugia Tune, slightly adapted to STAR data) [14, 15] prior  
33 and a GEANT-3 simulation of the STAR detector. The systematic uncertainties for data are taken  
34 as a quadrature sum resulting from the following sources: tracking efficiency (4%), tower gain  
35 calibration (3.8%), hadronic correction to the tower energy scale (described in [8]) and unfolding-  
36 related sources including varying the iteration parameter from 2 to 6 and the prior in the response  
37 matrix.

38 Figure 1 shows the fully unfolded  $z_g$  (left),  $R_g$  (middle) and  $M$  (right) distributions for jets with  
39  $20 < p_T < 25$  GeV/ $c$ , respectively. The STAR data are shown in the red filled star markers with the  
40 red shaded region corresponding to the overall systematic uncertainty. Leading order Monte Carlo  
41 (MC) generators such as PYTHIA-6 Perugia tune, PYTHIA-8 Monash [16], and Herwig-7 EE4C  
42 UE tune [17] in the blue, black and magenta lines are also plotted for comparison to the data. For  
43 the  $z_g$  observable, we also provide the symmetrized DGLAP splitting functions (noted as AP Q-Jet  
44 in the figure) at leading order in the red dashed lines for quark jets (with the splitting being similar  
45 for quark- and gluon-initiated jets). All the models studied reproduce the general trends seen in  
46 the data, particularly the dependence on the jet momenta leading to a steeper  $z_g$  distribution and a  
47 narrower  $R_g$ . As the jet mass is related to both the momentum and angular scales, the differences  
48 we see in both  $z_g$  and  $R_g$  carry over onto the mass with PYTHIA-8 and HERWIG-7 predicting  
49 larger and smaller masses respectively.

### 50 3. Iterative Jet-Substructure in p+p Collisions

51 The softdrop algorithm relies on an angular ordered clustered tree and in the previous section  
52 we presented the momentum and angular scale measurements at the first split. In applying the  
53 softdrop criterion iteratively [18] along the harder branch in the clustering tree, we are able to  
54 qualitatively reconstruct the splitting mechanics during jet clustering. Since the splits along the  
55 harder branch are ordered in their opening angle (by construction due to the angular ordering),  
56 a formation time argument can be invoked with representing the further splits as also occurring  
57 later in time during the parton shower. Such a measurement has the opportunity to experimentally  
58 reconstruct a parton shower in formation time and thus have the ability to look at snapshots in  
59 time coinciding with the individual splits. This feature is highly desirable in a tomographic study  
60 of the QGP since the jet as a whole is demonstrably modified and any experimental evidence  
61 of parton shower modifications point to medium properties that vary in formation time. STAR  
62 has taken the first step towards measuring the splitting mechanics, via the softdrop observables  
63  $z_g$  and  $R_g$  iteratively for the first (black), second (red) and third (blue) splits with their initiator  
64 prong's  $20 < p_T < 25$  GeV as shown in Fig 2. We observe a trend towards a flatter or more  
65 symmetric splitting at the third splits as compared to the first splits. These third splits are also much  
66 narrower as compared to the first and second splits. These distributions in data (star markers) are  
67 not fully corrected for detector effects and they are compared to PYTHIA-6+GEANT simulation  
68 (open circles) which are able to reproduce the distributions as seen in data.

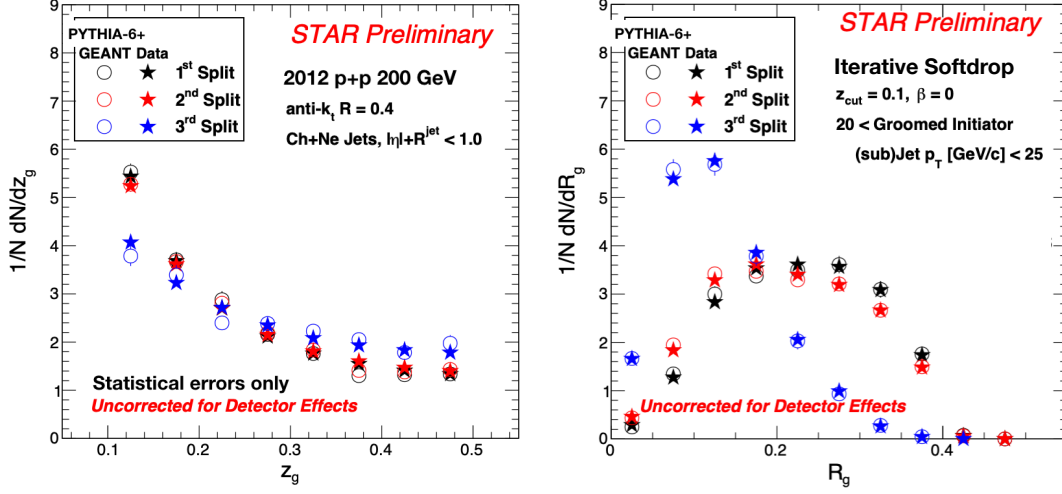


**Figure 2:** Measurement of the iterative  $z_g$  (left) and  $R_g$  (right) in p+p collisions at  $\sqrt{s} = 200$  GeV for anti-kt  $R=0.4$  Charged + Neutral jets at different splitting. Each split is selected to have its groomed initiator prong to have a transverse momenta  $20 < p_T < 25$  GeV. The first, second and third splits is shown in black, red and blue stars for the uncorrected data and compared with simulation in the open circles

#### 69 4. Jet Angular Scale in Au+Au Collisions

70 The Au+Au data used in these proceedings were collected during the 2007 run with its corre-  
 71 sponding reference p+p run in 2006 at  $\sqrt{s_{NN}} = 200$  GeV. Since the jet patch trigger is saturated in  
 72 an Au+Au event, we employ a high tower (HT) trigger, requiring at least one BEMC tower with  $E_T$   
 73  $> 5.4$  GeV. Event centrality in Au+Au is determined by the raw charged track multiplicity in the  
 74 TPC within  $|\eta| < 0.5$  and we show only events in the 0-20% centrality range. In Au+Au events,  
 75 we have two separate jet collections given by the Hardcore selection [8], where jets are clustered  
 76 with objects (tracks/towers) with  $p_T > 2$  GeV/c, and Matched jets which are clustered from the  
 77 constituent-subtracted [19] event with our nominal  $p_T > 0.2$  GeV/c for constituents, and are ge-  
 78 ometrically matched to the Hardcore jets ( $\Delta R < 0.4$ ). Further event selection criteria include a  
 79 minimum  $p_T$  requirement for Hardcore di-jets ( $p_T^{\text{Lead}} > 16, p_T^{\text{SubLead}} > 8$  GeV/c) and an azimuthal  
 80 angle ( $|\Delta\phi(\text{Lead}, \text{SubLead})| > 2\pi/3$ ) selection to focus on back-to-back di-jets.

81 In our studies, we found the groomed jet radii ( $R_g$ ) to be highly sensitive to the fluctuating  
 82 underlying event in Au+Au collisions and therefore we devised a new observable involving sub-  
 83 jets of a smaller radius reconstructed within the original jet (see here [13] for a recent theoretical  
 84 article demonstrating similar classes of observables). For our nominal anti- $k_t$  jets of  $R = 0.4$ , we  
 85 reconstruct an inclusive set of anti- $k_t$  sub-jets with  $R = 0.1$  from the original jet's constituents. An  
 86 absolute minimum sub-jet  $p_T$  requirement of 2.97 GeV/c is enforced in central Au+Au collisions  
 87 to reduce sensitivity to the background fluctuations. The two observables related to the momentum  
 88 and angular scales are then defined as follows  $z_{SJ} = \frac{\min(p_T^{SJ1}, p_T^{SJ2})}{p_T^{SJ1} + p_T^{SJ2}}$ , and  $\theta_{SJ} = \Delta R(SJ1, SJ2)$ , where  
 89  $SJ1, SJ2$  are the leading and sub-leading sub-jets, respectively.

90 For a meaningful comparison between Au+Au and a p+p reference, the effects of background  
 91 fluctuations and detector inefficiencies must be taken into account. To achieve this, HT-triggered

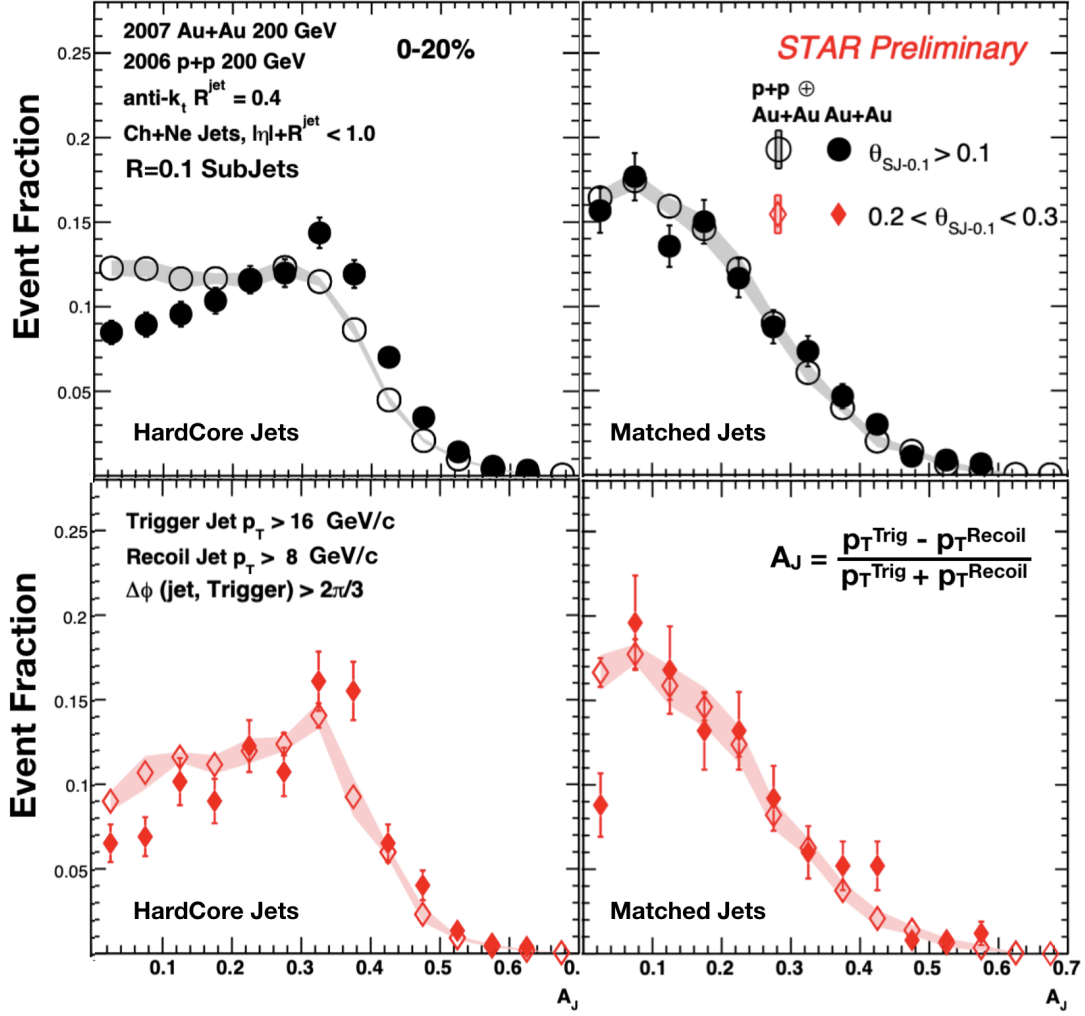


**Figure 3:** HardCore and Matched (left figure) di-jet asymmetry ( $|A_J|$ ) and the Matched recoil jet yield (right figure) along with the ratios shown in the bottom right panels. Markers are described in the text.

92 p+p data from 2006 is embedded into minimum bias Au+Au data (p+p $\oplus$ Au+Au) from 2007, in  
 93 the same centrality range (0-20%). During embedding, we account for the relative tracking effi-  
 94 ciency ( $90\% \pm 7\%$ ) and relative tower energy scale ( $100\% \pm 2\%$ ), with a one sigma variation taken  
 95 as systematic uncertainties. The TwoSubJet  $z_{SJ}$  and  $\theta_{SJ}$  distributions for constituent-subtracted  
 96 Matched recoil jets with  $R = 0.1$  sub-jets ( $SJ - 0.1$ ) recoiling off the trigger (selected with a  
 97  $|\Delta\phi(\text{jet, HT})| > 2\pi/3$ ), in the  $p_T$  range 10-20 GeV/c are observed to be similar in both Au+Au  
 98 and p+p $\oplus$ Au+Au [10]. We also observe a remarkable difference in the shape of  $z_{SJ}$  when com-  
 99 pared to that of the SoftDrop  $z_g$ , which is caused by selecting the core of the jet. The  $\theta_{SJ}$  for jets  
 100 within the considered  $p_T$  range peaks at small values and includes a natural lower cutoff at the  
 101 sub-jet radius and we now select jets based on this distribution.

102 Di-jet asymmetry for both HardCore and Matched jets (left panels) are shown in Fig. 4. The  
 103 right panels of Fig. 4 show the yield of Matched recoil jets normalized per di-jet for the different  
 104  $\theta_{SJ}$  selections and the ratios of Au+Au/p+p in the bottom panels. The black, blue and red markers

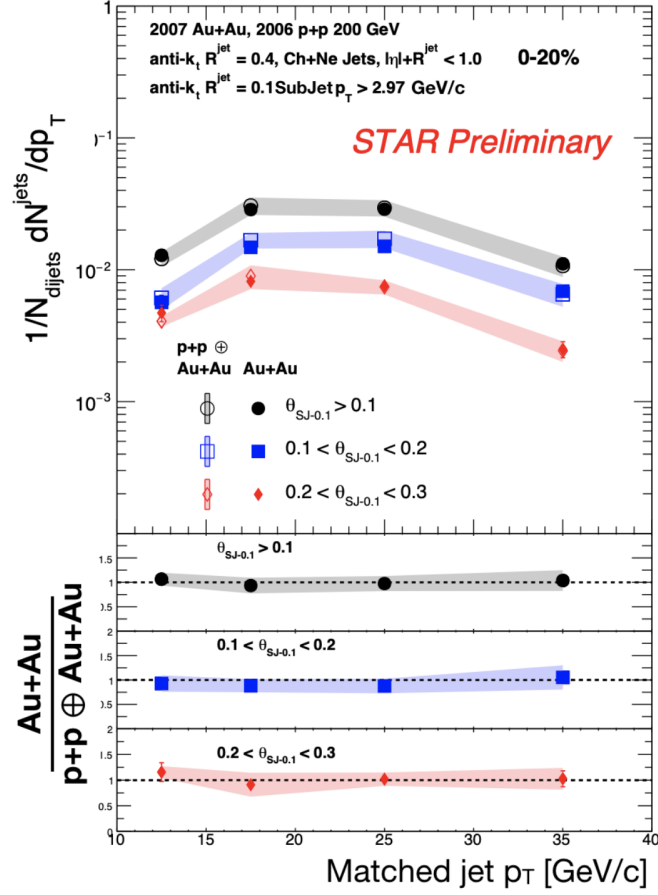


**Figure 4:** HardCore and Matched (left figure) di-jet asymmetry ( $|A_J|$ ) and the Matched recoil jet yield (right figure) along with the ratios shown in the bottom right panels. Markers are described in the text.

105 represent recoil jets with selections on  $\theta_{SJ}$  [0.1, 0.4], [0.1, 0.2] and [0.2, 0.3] for inclusive, narrow  
 106 and wide jets, respectively. We observe a clear di-jet imbalance indicating jet quenching effects in  
 107 the  $|A_J|$  distributions (comparing Au+Au to  $p+p \oplus Au+Au$ ) for all HardCore jets including the wide  
 108 angle jets. The Matched jets on the other hand are balanced at RHIC energies, as evident by ratios  
 109 in the bottom right panels consistent with unity. This is consistent with our earlier measurement [8].  
 110 We also note that wide angle jets are still balanced indicating no apparent distinction between wide  
 111 and narrow jets by the medium in our selection. Further detailed differential analyses are required  
 112 with the high statistics 2014 data set to extract the medium resolution scale or the coherence length  
 113 and the effect on standard jet quenching observables at RHIC energies.

## 114 5. Conclusions

115 STAR has presented the first fully unfolded jet substructure measurements including the Soft-  
 116 Drop  $z_g$  and  $R_g$  and jet Mass of inclusive jets with varying transverse momentum in p+p collisions  
 117 at  $\sqrt{s} = 200$  GeV. The measurements are overall reproduced by current leading order Monte Carlo  
 118 event generators for jets in our kinematic acceptance and reflect the momentum dependent narrow-

ing of jet structure. We also presented for the first time the iterative softdrop splitting observables at first, second and third splits. By comparing the  $z_g$  and  $R_g$  at various splits, we find that splits that occur further in the clustering tree have a larger  $z_g$  on average as opposed to those earlier in the tree. These measurements serve as a first look into an experimental measurement of parton shower of a jet at varying snapshots in time which can then be used to study medium properties in time dependent tomography. Due to the sensitivity of the SoftDrop observables to the Au+Au underlying event, we introduce and measure the TwoSubJet observables,  $z_{SJ}$  and  $\theta_{SJ}$  for  $R = 0.1$  anti- $k_t$  sub-jets as representing the momentum and angular scales of a jet in a heavy ion environment. We measure the di-jet momentum asymmetry and the recoil jet yield with the special di-jet selection at STAR and find that HardCore di-jets are imbalanced and Matched di-jets are balanced for jets of varying angular scales. We find no significant difference in the quenching phenomenon for both wide and narrow jets leading to the conclusion that these special jets do not undergo significantly different jet-medium interactions due to their varying angular scales.

## References

- [1] M. Connors, R. Reed, S. Salur, C. Nattrass, Rev. Mod. Phys. 90, (2018) 025005
- [2] Y. Mehtar Tani, K. Tywoniuk, Phys. Rev. D 98 (2018) 051501(R)
- [3] G. Altarelli, G. Parisi, Nucl. Phys. B126 (1977) 298-318
- [4] A. J. Larkoski, S. Marzani, G. Soyez, J. Thaler, JHEP 05 (2014) 146
- [5] A. J. Larkoski, S. Marzani, J. Thaler, Phys. Rev. D 91 (11) (2015) 111501
- [6] K. H. Ackermann et. al., Nucl. Instrum. Methods Phys. Res., Sect. A 499, (2003) 624
- [7] M. Cacciari, G. P. Salam, G. Soyez, JHEP 04 (2008) 005.
- [8] L. Adamczyk, et al., Phys. Rev. Lett. 119 (6) (2017) 062301
- [9] Nick Elsey for the STAR Collaboration PoS HardProbes2018, 87 (2018)
- [10] RKE for the STAR Collaboration, PoS HardProbes2018, 90 (2019)
- [11] T. Aye et. al. [hepunix.rl.ac.uk/~adye/software/unfold/RooUnfold.html](http://hepunix.rl.ac.uk/~adye/software/unfold/RooUnfold.html)
- [12] G. D'Agostini, arXiv:1010.0632
- [13] L. Apolinário, J. G. Milhano, M. Ploskon, X. Zhang, Eur. Phys. J. C78 (2018) no.6, 529
- [14] T. Sjostrand, S. Mrenna, P. Z. Skands, JHEP 05 (2006) 026
- [15] J. Adams et. al, arXiv: 1906.02740
- [16] T. Sjostrand, et. al., Comput. Phys. Commun. 191 (2015) 159-177.
- [17] M. Bahr, et al., Eur. Phys. J. C58 (2008) 639-707.
- [18] Christopher Frye, Andrew J. Larkoski, Jesse Thaler, Kevin Zhou, JHEP 09 (2017) 083
- [19] P. Berta, M. Spousta, D. W. Miller, R. Leitner, JHEP. 1406 (2014) 092